



**CALCULATION OF CHEMICAL POTENTIAL AND ACTIVITY  
COEFFICIENT OF TWO LAYERS OF CO<sub>2</sub> ADSORBED ON A  
GRAPHITE SURFACE**

Journal:	<i>Physical Chemistry Chemical Physics</i>
Manuscript ID:	CP-ART-08-2014-003782.R1
Article Type:	Paper
Date Submitted by the Author:	07-Nov-2014
Complete List of Authors:	Trinh, Thuat; NTNU, Department of Chemistry Bedeaux, Dick; NTNU, Chemistry Simon, Jean-Marc; Universit� de Bourgogne, Chemistry Kjelstrup, Signe; Norwegian University of Science and Technology, Natural Sciences

## ARTICLE

# CALCULATION OF CHEMICAL POTENTIAL AND ACTIVITY COEFFICIENT OF TWO LAYERS OF CO<sub>2</sub> ADSORBED ON A GRAPHITE SURFACE

Cite this: DOI: 10.1039/x0xx00000x

T.T. Trinh,<sup>a</sup> D. Bedeaux<sup>a</sup>, J.-M. Simon<sup>b</sup> and S. Kjelstrup<sup>a,c,\*</sup>Received 00th January 2014,  
Accepted 00th January 2014

DOI: 10.1039/x0xx00000x

www.rsc.org/

We study the adsorption of carbon dioxide at a graphite surface using the new Small System Method, and find that for the temperature range between 300K and 550K most relevant for CO<sub>2</sub> separation; adsorption takes place in two distinct thermodynamic layers defined according to Gibbs. We calculate the chemical potential, activity coefficient in both layers directly from the simulations. Based on thermodynamic relations, the entropy and enthalpy of the CO<sub>2</sub> adsorbed layers are also obtained. Their values indicate that there is a trade-off between entropy and enthalpy when a molecule chooses for one of the two layers. The first layer is a densely packed monolayer of relatively constant excess density with relatively large repulsive interactions and negative enthalpy. The second layer has an excess density varying with the temperature, an activity coefficient which also indicates repulsion, but to a much smaller degree than in the first layer. Results for activity coefficients, entropies and enthalpies can be used to model transport through and along graphitic membranes for carbon dioxide separation purposes.

## INTRODUCTION

Thanks to the definitions of excess variables by Gibbs already in 1877,<sup>1,2</sup> we are able to describe surfaces as thermodynamic systems. With the surface thickness integrated out, they are two-dimensional systems. Phase transformations,<sup>3</sup> formation of nanostructures,<sup>3,4</sup> metastable phases<sup>5</sup> or agglomerates<sup>6</sup> become special at surfaces or interfaces. Due to this a surface can pose a major barrier to transport<sup>7,8</sup> and catalyze chemical reactions.<sup>9</sup> In this entire context thermodynamic data are needed for modelling and understanding.

Thermodynamic knowledge of surfaces cannot be extrapolated from knowledge of homogeneous systems.<sup>3</sup> It is common to use the ideal Langmuir theory, or empirical variations of this theory, and Henry's law to describe adsorption of gas at internal or external surfaces.<sup>10-12</sup> Current experiments<sup>3</sup> do not give easy access to thermodynamic data for real surfaces. With the accuracy now obtainable for atomic force fields one may expect quantitative information from computational tools, among them Monte Carlo techniques.<sup>13,14</sup> To the best of our knowledge, the chemical potential or activity coefficient of a component in a surface have not yet been obtained from a single, simple molecular simulation.

We shall show in this work that this situation may change with the advent of the Small System Method. The method was

constructed by Schnell et al using Hill's thermodynamics for small systems.<sup>15,16</sup> An ensemble of small systems of varying sizes was examined, and scaling laws for the small system were derived from statistical mechanics. Fluctuation data were sampled, scaled appropriately and analyzed to find thermodynamic limit values. The method has now been used successfully to obtain Kirkwood – Buff integrals for mixtures and electrolytes,<sup>16</sup> reaction enthalpy<sup>17</sup> and accurate Fick diffusion coefficients in binary<sup>15</sup> and ternary mixtures.<sup>18</sup> More recently Collell and Galliero reported the thermodynamic correction factor of Lenard-Jones fluid in confinement using the Small System Method and a Langmuir isotherm model.<sup>19</sup>

We shall now demonstrate how the method can be used to find surface thermodynamic data, like the chemical potential, the enthalpy, the entropy, and the activity coefficient of a gas adsorbed to a surface, expanding on a first short communication.<sup>20</sup>

The adsorption of CO<sub>2</sub> on a graphite surface is relevant to graphitic membranes, which are promising cheap membranes for CO<sub>2</sub> separation purposes.<sup>21</sup> As a first case, we study the physisorption process



where (g) means gas phase, and (s) means gas adsorbed at the surface. We shall see that new details emerge for the state denoted (s): Adsorption takes place in two distinct layers with different enthalpy and entropy in the temperature range considered (300K-500K). The first layer has low entropy with less mobile molecules, while the second layer has higher entropy contains less bound molecules. The layers are not filled sequentially, but maintain states which are in equilibrium with each other.

## METHODS

### Thermodynamic relations

The chemical potential for a gas adsorbed to a surface in layer no  $i$  ( $i=1,2$ ) is:

$$\mu_i^s = \mu_i^{s,0} + RT \ln a_i^s = \mu_i^{s,0} + RT \ln \gamma_i^s \frac{C_i^s}{C_i^{s,0}} \quad (2)$$

Here  $\mu_i^{s,0}$  is the standard chemical potential,  $a_i^s$  is the (dimensionless) activity of the adsorbed phase,  $C_i^s$  is the surface excess concentration, and  $\gamma_i^s$  is the activity coefficient. The standard state is normally chosen as the hypothetical ideal state having  $\gamma_i^s=1$  at layer saturation  $C_i^{s,0}$  (given as particles per  $\text{nm}^2$ ). Subscript  $i$  refers to the layer number. The entropy follows from the standard relation  $S=-(\text{d}\mu/\text{d}T)$ :

$$S_i^s = S_i^{s,0} - R \ln \gamma_i^s \frac{C_i^s}{C_i^{s,0}} \quad (3)$$

The enthalpy of layer  $i$  is accordingly:

$$H_i^s = \mu_i^s + TS_i^s \quad (4)$$

We shall determine the variables in these equations for adsorption (1). Following Gibbs, the total adsorption  $C^s$  is defined as the total surface excess concentration. For the layer  $i$ , we use two surfaces  $\alpha$  and  $\beta$  between the two bulk phases. The total adsorption is then the sum of the adsorptions in the layers

$$C^s = C_1^s + C_2^s = \int_0^\alpha C(z) dz + \int_\alpha^\beta C(z) dz \quad (5)$$

where  $C(z)$  is the concentration of the  $\text{CO}_2$  molecules. For the definition of  $\alpha$  and  $\beta$ , we refer to the results and discussion section.

A thermodynamic state is characterized, once the standard state and activity coefficients of components are known as a function of temperature, cf. equation (2-5). The thermodynamic correction factor, easily accessible by the Small System Method, can be used to find this information. For constant temperature  $T$  and surface area  $A$  the thermodynamic factor is defined by:

$$\Gamma^s = 1 + \left( \frac{\partial \ln \gamma^s}{\partial \ln C^s} \right)_{T,A} \quad (6)$$

We determine the activity coefficient by integrating equation (6) from zero adsorption:

$$\int_1^{\gamma^s} d \ln \gamma^s = \int_0^{C^s} (\Gamma^s - 1) d \ln C^s \quad (7)$$

When  $C^s \rightarrow 0$ , there is no interaction between particles, meaning that  $\gamma^s = 1$ .

For the gas phase the chemical potential is:

$$\mu^g = \mu^{g,0} + RT \ln a^g = \mu^{g,0} + RT \ln \frac{P}{P^0} \quad (8)$$

where  $a^g$  is the activity of the gas and  $P$  is the pressure of the gas, which is taken to be ideal. If the gas is non-ideal  $P$  must be replaced by the fugacity. We know the standard state value for the gas phase from standard tables, and want to determine the value for the adsorbed state for a chosen standard state. We choose an ideal state with full coverage. This is a hypothetical state with activity coefficient of unity. The state is obtained by extrapolating Henry's law to the state of full coverage.

We will see that the second layer behaves according to Henry's law for the whole pressure range (See SI). This makes it convenient to use the second layer in the definition of the surface standard state. The first layer has a much smaller pressure range where Henry's law applies, and the extrapolation becomes uncertain. Henry's law can be written:

$$K_H = \frac{C_2^s}{C_2^{s,0}} \frac{P^0}{P_2}, \quad \frac{C_2^s}{C_2^{s,0}} = K_H \frac{P_2}{P^0} \quad (9)$$

Where  $K_H$  is the temperature dependent, Henry's law constant, and  $C_2^{s,0}$  is a monolayer coverage of the surface. The law assumes that  $\gamma_i^s = 1$  for low adsorptions. For adsorbed  $\text{CO}_2$  in layer 2 in equilibrium with the gas, we have under ideal conditions

$$\mu_2^s = \mu_2^{s,0} + RT \ln \frac{C_2^s}{C_2^{s,0}} = \mu_2^{s,0} + RT \ln K_H \frac{P_2}{P^0} \quad (10)$$

With equilibrium between the layers we have

$$\mu_1^s = \mu_2^s = \mu^g \quad (11)$$

The last equality means that

$$\mu_2^{s,0} + RT \ln \frac{P_2}{P^0} = \mu_2^{s,0} + RT \ln K_H \frac{P_2}{P^0} \quad (12)$$

$$\mu_2^{s,0} = \mu_2^{g,0} - RT \ln K_H \quad (13)$$

This expression enables us to calculate the standard state chemical potential of the surface as a function of temperature, in terms of known quantities. When the standard state is known we can use the results for the activity coefficient and concentration to calculate the chemical potential under real conditions.

### The Small System Method applied to surface adsorption

In the Small System Method, we make use of the relation between the inverse of thermodynamic correction factor and fluctuations in particle number  $N$ . For a surface, the expression becomes

$$\frac{1}{\Gamma} = \left[ \frac{\langle N^2 \rangle - \langle N \rangle^2}{\langle N \rangle} \right]_{T, \mu, A} \quad (14)$$

In the method we sample fluctuations inside a reservoir. The reservoir is created as a large rectangular box with periodic boundary conditions. The temperature and chemical potential in the box are controlled via the boundaries. Inside the box, we sample open systems with area  $A$ . The thickness of the sampling box is set equal to the thickness of the surface (see below). The thermodynamic factor, so obtained, refers to a small system at constant  $T$ ,  $\mu$  and  $A$ . Small system properties depend on the size of the reservoir, unlike what properties of macroscopic systems do.

The shape of the small system used for sampling is important. A disk is chosen here to avoid line and nook energies. The area of the sampling system is varied in a systematic way, varying the radius of the disk,  $L$ . The smallest radius can be so small that it allows only one molecule inside the disk; the largest radius can allow around 20-30 molecules, which is still small for molecular simulations (leading to the name of the method, the small system method). The inverse thermodynamic factor was found to be a linear function of the inverse radius, see refs, <sup>22-24</sup> in a particular range, to be found for each case:

$$\frac{1}{\Gamma} = \frac{1}{\Gamma^s} \left[ 1 + \frac{B}{L} \right] \quad (15)$$

Here  $B$  is a small system specific constant and superscript  $s$  means a value in the thermodynamic limit. By extrapolating the linear regime to the thermodynamic limit, we obtain the wanted quantity  $\Gamma^s$ .

## SIMULATION DETAILS

### Carbon dioxide and graphite models

The system consisted of sheets of graphite and CO<sub>2</sub> molecules. The graphite was made from 5 sheets of graphene without any defects. The stacking of the graphite layer was in the ABA manner. We oriented the sheets in the box such that the sheet surfaces were perpendicular to the  $z$ -axis. The distance from the graphite surface was measured along this axis, taking the equimolar surface of graphite as zero. The graphite layers were fixed in space, still yielding good results for adsorption and diffusion of gas on the surface.<sup>25, 26</sup> A rigid body model, TraPPE, was used for CO<sub>2</sub>.<sup>27</sup> The intermolecular potential between CO<sub>2</sub> – CO<sub>2</sub> was a shifted and truncated 12-6 Lennard-Jones (LJ) potential<sup>14</sup> with long-range Coulomb interactions, which were dealt with using the Ewald summation technique.<sup>14</sup>

The interaction between CO<sub>2</sub> and the C-atoms of graphite was similarly described by a LJ potential. Details of parameters for the simulation were given earlier.<sup>25</sup> They have been confirmed to yield an accurate adsorption energy for CO<sub>2</sub> on a graphite surface.<sup>25</sup> Parameters, taken from the DREIDING<sup>28</sup> and TraPPE<sup>27</sup> force fields, are listed in Table 1. A snapshot of the system is given in Fig. 1, showing graphite at 500 K with CO<sub>2</sub> in a relatively dense gas and in an adsorbed state.

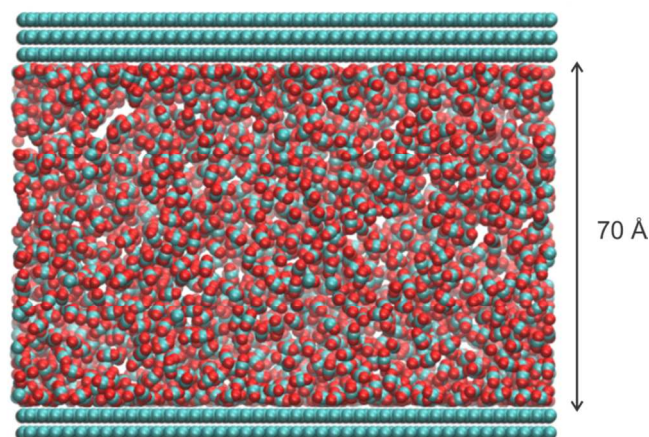


Figure 1. Snapshot of system showing CO<sub>2</sub> in the gas phase at a relatively high density, and adsorbed on a graphite surface at 500 K. The number of CO<sub>2</sub> particles in the system is  $N_{\text{CO}_2}=2800$ . (System X4, see text). The green and red colours represent carbon and oxygen atoms, respectively.

Classical molecular dynamics (MD) simulations were performed using the LAMMPS package.<sup>29</sup>

Table 1. LJ potential parameters used in simulation TraPPE<sup>27</sup> and DREIDING<sup>28</sup> force fields.

Atom	Radius $\sigma$ (Å)	Depth of potential $\epsilon/k_B$ (K)	Charge (e)
C (in CO <sub>2</sub> )	2.80	27	0.70
O (in CO <sub>2</sub> )	3.05	79	-0.35
C (graphite)	3.34	26	0.00

### The reservoir: Periodic boundary conditions and size

Periodic boundary conditions were used for the reservoir in all directions. The simulation had time steps of 0.001ps. The initial configuration was constructed by randomly distributing CO<sub>2</sub> molecules above the graphite surface. The system was equilibrated during 2000 ps by runs with constant  $N_{\text{tot}}V_{\text{tot}}T$  using Nosé-Hoover thermostats.<sup>30</sup> To ensure that the system in equilibrium, we have checked the convergence of the temperatures within 1% of the expected values. (See SI).

In order to check the range of validity of equation (15), the reservoir size was varied. The reservoir has to be large enough compared to the sampling system. For a hard sphere system, we found that a suitable reservoir (parallel to the surface) had a length 20 times the hard sphere diameter.<sup>23, 24</sup> Three sizes were therefore chosen for the reservoir, denoted X1, X4 and X9. The

simulation box size of X1 was ( $a=42\text{\AA}$ ,  $b=54\text{\AA}$ ,  $c=84\text{\AA}$ ), for the X4 box it was: ( $2a$ ,  $2b$ ,  $c$ ), while for the X9 box it was ( $3a$ ,  $3b$ ,  $c$ ). The gas concentration was constant in these runs, meaning that the number of  $\text{CO}_2$  molecule in X4 (X9) was 4 (9) times larger than in X1. About ten runs were simulated for each box showing a variation in the inverse thermodynamic correction factor from X1 to X4, while the X4 system gave identical results to the X9 system, see Fig. S3. The box size X4 was therefore taken as being sufficiently large, and we will not refer to X4 explicitly.

### Case studies

In order to examine adsorption of  $\text{CO}_2$  on graphite under microcanonical ensemble conditions, we performed 2000 ps runs in a reservoir at thermal equilibrium. The disk used to sample fluctuations was described above. We varied the radius  $L$  from 1.3 to 20  $\text{\AA}$ , sampling randomly 30 disks across the graphite surface. The total number of frames was 10000. Hence, the value of  $\Gamma^s$  for each  $L$  was obtained from the statistics of 300 000 samples.<sup>22, 24</sup> The sampling was done for temperatures ranging from 300K to 550K, and for a number of  $\text{CO}_2$  particles in the box, varying from 200 to 2800 (corresponding to a pressure range of 1- 60 bar at 300K).

## RESULTS AND DISCUSSION

### Adsorptions

We describe first how we find the adsorptions  $C_1^s$  and  $C_2^s$  for each layer. The total adsorption is then  $C^s = C_1^s + C_2^s$ . We find the thermodynamic factor, the activity coefficients as function of adsorption from equation (7), the chemical potential as a function of adsorption and temperature from equation (2), and accordingly, the entropy and enthalpy from equations (3,4).

The adsorption (excess concentration) of  $\text{CO}_2$  was found from Figure 2. The figure shows the density of  $\text{CO}_2$  molecules as a function of the distance to graphite surface, and is a quantification of snapshots like the one showed in Fig. 1. We observe in both figures that  $\text{CO}_2$  forms two layers on the graphitic surface. In Figure 2, we see a layer around the first peak which extends from the graphite surface to position  $\alpha$ , while a second peak extends from  $\alpha$  to  $\beta$ . We refer to the integral in equation (5) from the first peak as the first layer (layer 1), while the corresponding integral related to the second peak, is called the second layer (layer 2) with respect to the graphite.

The position extension of the first peak stays around 5  $\text{\AA}$  and cover almost the length of the molecule, 5.4  $\text{\AA}$ . The snapshot shows that most of the carbon dioxide molecules are lying parallel to the surface, with a height more like the diameter of an oxygen ion, 3.6  $\text{\AA}$ . A thickness of 5  $\text{\AA}$  will include some molecules which are standing almost perpendicular, slightly tilted with respect to the surface, and such molecules can also be found by visual inspection of Fig. 1. It is interesting that the position of plane  $\alpha$  is always near 5 $\text{\AA}$ , independent of the

temperature. This reflects that molecules are either lying or standing in the first layer. The attractive forces of the graphite, do not reach above the layer, which seems to be central for this layer.

The fact that the second layer starts to be filled before the first layer is full, motivates a division of the whole surface into two layers. The second layer, which extends from  $\alpha$  to  $\beta$ , appears rather different from the first. We see from Fig. 2 that the position of the plane  $\beta$  varies with temperature, unlike the plane  $\alpha$ . For the system with 2800  $\text{CO}_2$  molecules  $\beta$  is smaller at 500K than at 350K. The second layer is more diffuse. The attractive forces are able to keep the molecules within the surface when molecular kinetic energy becomes larger. The adsorption of the  $\text{CO}_2$  on graphite is always higher at low temperature in both layers, meaning that this kind of trade-off between kinetic and potential energies applies in both cases.

Two layers of  $\text{CO}_2$  was reported previously in simulations at 323K on a graphite surface.<sup>31</sup> The number of layer strongly depends on temperature range. For example at high temperature (700K) a mostly that only single layer is observed, and at low temperature (250K) multilayer is formed (see SI, Fig. S2). However, we are interested in the temperature range of 300K-550K which is similar to experimental conditions of  $\text{CO}_2$  adsorption and separation process.<sup>32-34</sup> In the temperature range considered,  $\text{CO}_2$  forms two layers on a graphite surface.

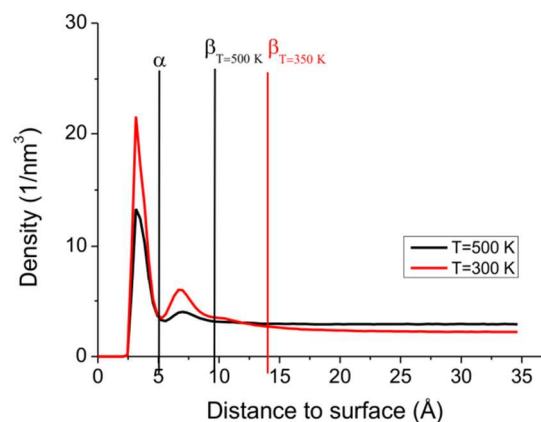


Figure 2. The density of  $\text{CO}_2$  molecules as a function of distance to the surface in a reservoir with  $N_{\text{CO}_2}=2800$ . The temperatures are 500K and 350K. We distinguish between three zones, from 0- $\alpha$ : first adsorbed layer,  $\alpha$ - $\beta$ : second adsorbed layer, above  $\beta$ : gas phase. The first layer extends to around 5 $\text{\AA}$ . The thickness of the second layer is larger at 350K than that at 500K.

The fraction of molecules in the first layer,  $C_1^s / (C_1^s + C_2^s)$ , is plotted in Fig. S4 as a function the total adsorption at various temperatures. The first layer has always more than half of the total adsorption independent of temperature. The fraction is larger, the lower the temperature is, but does not exceed 0.9. The fraction decreases with increasing total adsorption, because the first layer gets saturated, while the second layer keeps growing. Full coverage (maximum adsorption) of the first layer is obtained at 300 K with  $C_1^{s,0} = 12.5$  molecules/( $\text{nm}^2$ ). We shall therefore chose as standard state,  $C_1^{s,0} = 12.5$  molecules/( $\text{nm}^2$ )

not only for the first, but also for the second layer and the combined layers. This coverage corresponds to 0.31 CO<sub>2</sub> molecule per graphite surface carbon atom.

### The thermodynamic correction factor

Typical results of the calculation of  $\Gamma^s$  for the small systems, using equation (10) are shown in Fig. 3 (for  $N_{\text{CO}_2} = 2800$  at 500K). The inverse thermodynamic factor is plotted for the second and first layer and their combination, versus  $1/L$ . The curves approach unity as expected, when  $1/L$  increases. This is the small system limit, which has one or zero particle in the sampling system. In order to find the thermodynamic limit-value we apply linear regression to points in the interval  $0.1 < 1/L < 0.4$  and extrapolate the line to large  $L$ . The region used for extrapolation coincides with the region found earlier.<sup>22, 24</sup>

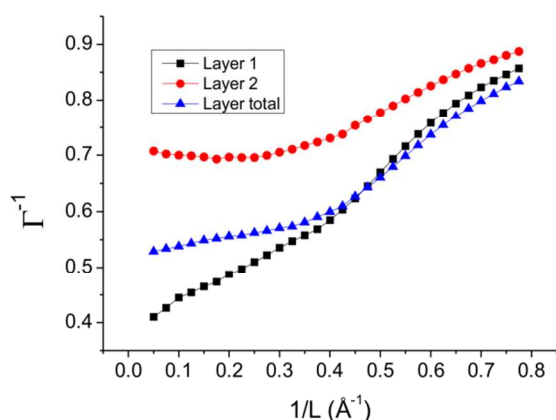


Figure 3. Inverse thermodynamic factor as a function of inverse disk radius for various layers of CO<sub>2</sub> adsorbed on the graphite surface. The temperature is 500 K and the number of molecules is  $N_{\text{CO}_2} = 2800$ .

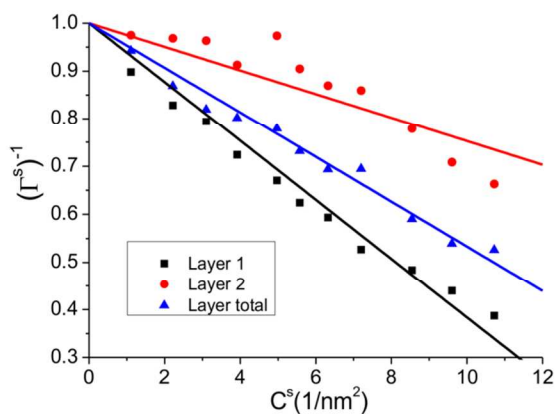


Figure 4. Thermodynamic limit values for  $\Gamma^{-1}$  in the first, second and total CO<sub>2</sub> layer on graphite at 500 K. A straight line is fitted to the results and forced through 1 on the y-axis.

The thermodynamic limit values of the inverse thermodynamic correction factors  $1/\Gamma^s$  of the different layers were determined as function of the adsorption in the layer in question and the

temperature. A typical example is shown in Fig. 4 for  $T=500\text{K}$ . The first layer has always the smallest  $1/\Gamma^s$ , while the second layer has the biggest values of  $1/\Gamma^s$ . It is interesting to see that  $1/\Gamma^s$  decreases more or less linearly with the adsorption in each layer. The first layer and the total layer follow the straight line nicely, while the scatter around the line of the second layer is larger. All curves must extrapolate to a thermodynamic correction factor equal to 1, when the adsorption goes to zero, and this is found. Data for all first and second layers are presented in Fig. S5 for all conditions investigated. The results for the first layer follow a straight line remarkably well. The results for the second layers become in general closer to a straight line at high temperatures ( $T=450\text{-}550\text{K}$ ). The second layer is thicker at low temperature, containing more CO<sub>2</sub> (Figure 2) and give better statistics. The relation between  $1/\Gamma^s$  of the total layer and the total adsorption is quite linear with the total adsorption, masking the special nature of the second layer.

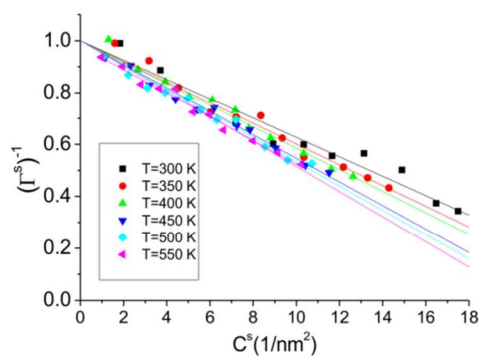


Figure 5. The inverse thermodynamic correction factor  $\Gamma^{-1}$  of the total layer as a function of the total adsorption of CO<sub>2</sub> on graphite. Results are shown for various temperatures.

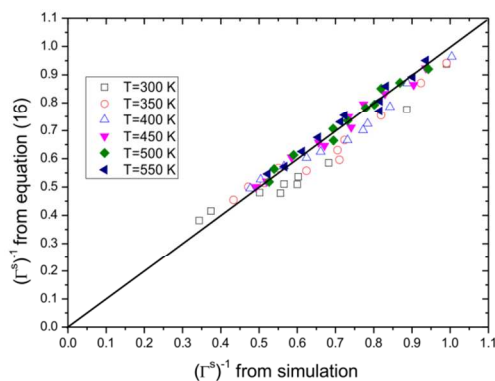


Figure 6. The inverse of thermodynamic correction factor from equation (16) and from simulation data.

Given the linear dependencies of the total layer observed in Fig. 5, one may expect that the inverse thermodynamic factor of the total layer can be found by averaging the contributions from the two layers:

$$\Gamma_{tot}^{-1} = \frac{C_1^s \Gamma_1^{-1} + C_2^s \Gamma_2^{-1}}{C_1^s + C_2^s} \quad (16)$$

This formula was tested and the results are shown in Fig. 6. We see that  $1/\Gamma^s$  indeed can be obtained using a weighted average of  $1/\Gamma_1^s$  and  $1/\Gamma_2^s$ , especially at high temperatures  $T = (450-550\text{K})$ . The average values from the MD simulation compare well to the ones calculated from equation (16).

### The activity coefficients for carbon dioxide in the surfaces

The activity coefficients of the surface were obtained from equation (7) and are shown in Fig. 7. All coefficients approach 1 as expected at low density, some with more noise than others. With one exception (second layer, 300 K) all activity coefficients are larger than unity and are increasing with the adsorption in question. The results at 500 K are typical, see Fig. S6. The increase in the first layer is larger than in the second layer and therefore larger than in the total layer. This reflects that the molecules are further apart in the second layer than in the first, making repulsive forces less relevant in the second than to the first layer. The molecules do not adsorb, unless the surface binding energy can overcome the repulsion, however.

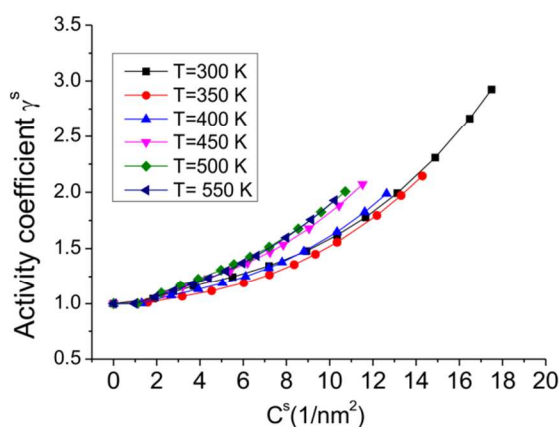


Figure 7. Activity coefficient of the total surface layer as a function of total surface adsorption at different temperatures.

Fig. 7 shows the total layer activity coefficient as a function of total surface adsorption at different temperatures. The curves were fitted to second order polynomials, one curve for each temperature:

$$\gamma_i = 1 + aC_i^s + b(C_i^s)^2 \quad (17)$$

The fitting parameters are given in Table 2. The regression coefficient is excellent ( $> 0.99$ ). This result may be useful for thermodynamic modelling of the total  $\text{CO}_2$  adsorbed on a graphitic surface.

Table 2. Parameters to describe the total layer activity coefficient by the empirical equation (17). The regression coefficient was always 0.99 or better.

$T(\text{K})$	$b$	$a$
300	0.0060	0.0005
350	0.0059	0.0054
400	0.0055	0.0066
450	0.0059	0.0233
500	0.0057	0.0320
550	0.0067	0.0216

### The chemical potential of the surface adsorbed gas

Using the relevant activity coefficient, and  $C^{0,s} = C_1^{0,s} = C_2^{0,s} = 12.5$  molecules/ $\text{nm}^2$ , we next used equation (13) to find the chemical potential of standard state for each layer and for the total layer. The adsorption of the first layer and the second layer is presented in Fig. S7. The standard state value,  $\mu_s^0$ , was found from equation (13) as described in the method section. The data are listed in Table 3 for all layers. We see how the value varies with temperature. The chemical potential difference for the total layer is presented in Fig. 8 for different temperatures. The results for the single layers look similarly.

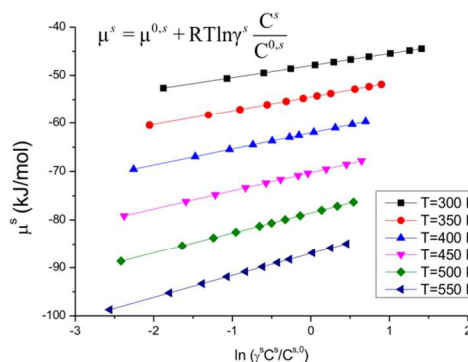


Figure 8. Chemical potential of  $\text{CO}_2$  on a graphite surface as a function of  $\ln \gamma^s C^s / C^{s,0}$  at different temperatures.

Table 3. Standard chemical potentials (in kJ/mol) as a function of temperature for single and total layers of  $\text{CO}_2$  adsorbed on a graphitic surface.

Temperature (K)	$\mu^{0,s}$	$\mu_1^{0,s}$	$\mu_2^{0,s}$
300	-48.24	-43.52	-47.96
350	-54.35	-50.03	-54.49
400	-61.60	-57.26	-62.05
450	-68.81	-64.92	-70.26
500	-76.46	-72.91	-78.57
550	-84.49	-81.18	-87.02

Table 4 Thermodynamic data for standard state adsorption of carbon dioxide at a graphite surface at T=298 K. The uncertainty in the determinations is on the average 3%

T=298 K	Total layer	First layer	Second layer	Graphite <sup>a</sup>	CO <sub>2</sub> gas <sup>a</sup>
$\mu_i^{0,s}$ (kJ/mol)	-47±1	-47±1	-42±1	/	/
$S_i^{0,s}$ (J/mol K)	157±3	145±3	155±3	5.74	213.78
$H_i^{0,s}$ (kJ/mol)	0±1	-4±1	3±1	1.05	9.36

a: values from ref<sup>35</sup>

### Two distinct layers of CO<sub>2</sub> in equilibrium

The thermodynamic data that we have determined for the total layer of adsorbed gas are reasonable. The standard chemical potential is negative, indicating that adsorption is favorable in the standard state, in spite of a reduction in the entropy from the gas phase to the surface.

We have furthermore seen that we can distinguish between two separate thermodynamically defined layers of carbon dioxide within the whole layer on the graphite surface in the temperature range considered. Each layer has its own thermodynamic properties. We see from Table 4, that the first layer entropy is relatively small compared to the gas entropy of CO<sub>2</sub>. The low entropy represented is overcome by a relatively favorable enthalpy in the layer. The combination explains the negative standard chemical potential. The second layer has larger entropy than the first layer. This layer is therefore stable with a smaller enthalpy. This discussion refers to standard state values, but applies also to other states.

It is interesting that the total layer properties are in between the properties of the single layers. The results obtained for the separate layers are internally consistent. Consider more specifically the second and first layers of CO<sub>2</sub>. Each layer has its own chemical potential, as stated in equation (2). By introducing the expression for each layer into equation (11), we obtain

$$\left(\frac{C_1^s}{C_2^s}\right) = \left(\frac{\gamma_2^s}{\gamma_1^s}\right) \exp\left(\frac{\mu_2^{s,0} - \mu_1^{s,0}}{RT}\right) \quad (18)$$

By plotting the left hand side versus the ratio of activity coefficients, fitting the plot to a straight line, we calculated  $\mu_2^{s,0} - \mu_1^{s,0}$  from the slope as a function of temperature. The difference in standard chemical potentials was consistent with the difference obtained from the data in Table 4.

### Entropy and Enthalpy of CO<sub>2</sub> layers

The entropy was also plotted as function of  $\ln(C^s \gamma^s)$  (the concentration is in the units of the standard concentration) in

Fig. 9, following equation (3). The linear fit in Fig. 9 gave a slope close to the value of the gas constant as expected. We also find the entropy of layer is compatible with value that found in Table 4, meaning that our data are internally consistent.

The standard enthalpy at 298 K was calculated from equation (4), giving  $H^0 = 0 \pm 1$  kJ/mol. The other data corresponding to these determinations for the first and second layers are given in Table 4. The adsorption enthalpy of CO<sub>2</sub> gas on graphite surface at standard state can be calculated from

$$\Delta H_{ads}^0 = H_{CO_2(adsorbed)}^0 - (H_{graphite}^0 + H_{CO_2(gas)}^0) \quad (19)$$

We substituted values from Table 4 using experimental values for graphite and CO<sub>2</sub> gas and obtained  $-10 \pm 1$  kJ/mol, which is in agreement with the experimental value for adsorption enthalpy of CO<sub>2</sub> gas in activated carbon.<sup>32, 36</sup>

It is interesting to have a closer look at the enthalpy of the surface layer (Table 4). The layer data give more information, with more negative values for the first layer, and slightly positive values for the second layer. The enthalpy of the total layer varying between -2 and 2 kJ/mol. (see Fig. 10). The scatter in the figure may reflect that the data are sampled at different temperatures.

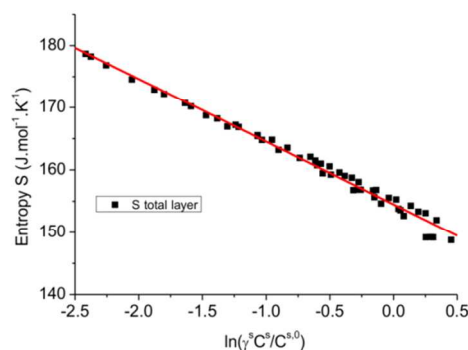


Figure 9. Entropy for total adsorption of carbon dioxide on graphite, vs  $\ln(\gamma^s C^s / C^{s,0})$  in the temperature interval 300 – 550 K.

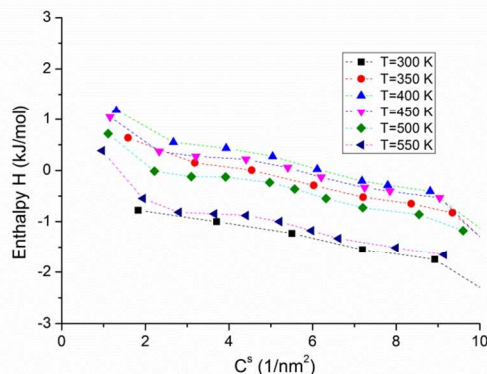


Figure 10. Enthalpy of total adsorbed carbon dioxide on a graphite surface as a function of the total adsorption.

## CONCLUSIONS

We have demonstrated how to use the recently developed Small System Method to calculate a consistent set of thermodynamic data for the surface adsorbed gas. For carbon dioxide adsorbed to graphite, we determined the chemical potential, the activity coefficient, the entropy and enthalpy, directly from Molecular Dynamics simulations. Closer inspection of data revealed that we can speak of two, not one layer of adsorbed gas, with distinct properties in the temperature range from 300K to 550K. The second layer has larger entropy than the first layer. The two layers are in equilibrium with each other, meaning that further lowering of the entropy can take place, if the enthalpy can compensate for the change in entropy. Such information is invaluable in the modelling and explanation of most surface processes. The filling of layers occurs in this trade-off situation. The standard state data of each surface layer was determined and empirical relations were given for activity coefficients. Extensions to other surfaces should be straightforward and give interesting perspectives in view of the literature for surface phase transitions.

## Acknowledgements

The authors acknowledge The Research Council of Norway RCN project no 209337 and The Faculty of Natural Science and Technology, Norwegian University of Science and Technology (NTNU) for financial support. The calculation power is granted by The Norwegian Metacenter for Computational Science (NOTUR) project nn9229k and nn4504k.

## Notes and references

a Department of Chemistry, Norwegian University of Science and Technology, Trondheim, Norway.

b Laboratoire Interdisciplinaire Carnot de Bourgogne, UMR-6303 CNRS-Université de Bourgogne, Dijon, France.

c Department of Process and Energy Laboratory, Delft University of Technology, Delft, The Netherlands.

\*Email: [Signe.Kjelstrup@ntnu.no](mailto:Signe.Kjelstrup@ntnu.no)

Electronic supplementary information (ESI) available: average temperature and potential energy during simulation, adsorption and concentration of CO<sub>2</sub> at different temperatures, activity coefficient of adsorbed layer of CO<sub>2</sub>. See DOI: XXX

- J. W. Gibbs, *The scientific papers of JW Gibbs, vol. 1*, Dover, New York, 1961.
- J. W. Gibbs, *On the equilibrium of heterogeneous substances*, Connecticut Academy of Arts and Sciences, 1877.
- L. P. H. Jeurgens, Z. M. Wang and E. J. Mittemeijer, *Int. J. Mater. Res.*, 2009, **100**, 1281-1307.
- F. Costache, S. Kouteva-Arguirova and J. Reif, *Applied Physics A*, 2004, **79**, 1429-1432.
- R. Bradley Shumbera, H. H. Kan and J. F. Weaver, *Surf. Sci.*, 2007, **601**, 235-246.
- D. J. Srolovitz and M. G. Goldiner, *Jom-J Min Met Mat S*, 1995, **47**, 31-&.
- I. Inzoli, J. M. Simon and S. Kjelstrup, *Langmuir*, 2009, **25**, 1518-1525.
- I. Inzoli, J. M. Simon, D. Bedeaux and S. Kjelstrup, *J. Phys. Chem. B*, 2008, **112**, 14937-14951.
- M. P. Cox, G. Ertl, R. Imbihl and J. Rustig, *Surf. Sci.*, 1983, **134**, L517-L523.
- J. Rouquerol, F. Rouquerol, P. Llewellyn, G. Maurin and K. S. Sing, *Adsorption by powders and porous solids: principles, methodology and applications*, Academic press, 2013.
- I. Langmuir, *J. Am. Chem. Soc.*, 1918, **40**, 1361-1403.
- T. S. van Erp, T. T. Trinh, S. Kjelstrup and K. Glavatskiy, *Frontiers in Physics*, 2013, **1**.
- D. Frenkel and B. Smit, *Understanding molecular simulation: from algorithms to applications*, Academic press, 2002.
- M. P. Allen and D. J. Tildesley, *Computer simulation of liquids*, Oxford university press, 1989.
- X. Liu, S. K. Schnell, J. M. Simon, D. Bedeaux, S. Kjelstrup, A. Bardow and T. J. Vlugt, *J. Phys. Chem. B*, 2011, **115**, 12921-12929.
- P. Krüger, S. K. Schnell, D. Bedeaux, S. Kjelstrup, T. J. Vlugt and J.-M. Simon, *J. Phys. Chem. Lett.*, 2012, **4**, 235-238.
- R. Skorpa, J.-M. Simon, D. Bedeaux and S. Kjelstrup, *Phys. Chem. Chem. Phys.*, 2014.
- X. Liu, A. Martin-Calvo, E. McGarrity, S. K. Schnell, S. Calero, J.-M. Simon, D. Bedeaux, S. Kjelstrup, A. Bardow and T. J. Vlugt, *Ind. Eng. Chem. Res.*, 2012, **51**, 10247-10258.
- J. Collell and G. Galliero, *J. Chem. Phys.*, 2014, **140**, 194702.
- T. Trinh, D. Bedeaux, J.-M. Simon and S. Kjelstrup, *Chem. Phys. Lett.*, 2014, **612**, 214.
- X. He, J. Arvid Lie, E. Sheridan and M.-B. Hägg, *Energy Procedia*, 2009, **1**, 261-268.
- S. K. Schnell, X. Liu, J.-M. Simon, A. Bardow, D. Bedeaux, T. J. H. Vlugt and S. Kjelstrup, *J. Phys. Chem. B*, 2011, **115**, 10911-10918.
- S. K. Schnell, T. J. H. Vlugt, J.-M. Simon, D. Bedeaux and S. Kjelstrup, *Chem. Phys. Lett.*, 2011, **504**, 199-201.
- S. K. Schnell, T. J. H. Vlugt, J.-M. Simon, D. Bedeaux and S. Kjelstrup, *Mol. Phys.*, 2011, **110**, 1069-1079.
- T. T. Trinh, T. J. Vlugt, M. B. Hagg, D. Bedeaux and S. Kjelstrup, *Front Chem*, 2013, **1**, 38.
- T. S. van Erp, T. T. Trinh, S. Kjelstrup and K. Glavatskiy, *Frontiers in Physics*, 2014, **1**, 36.
- J. J. Potoff and J. I. Siepmann, *AIChE J.*, 2001, **47**, 1676-1682.
- S. L. Mayo, B. D. Olafson and W. A. Goddard, *J. Phys. Chem.*, 1990, **94**, 8897-8909.
- S. Plimpton, P. Crozier and A. Thompson, *LAMMPS-large-scale atomic/molecular massively parallel simulator*, (2007).
- G. J. Martyna, M. L. Klein and M. Tuckerman, *J. Chem. Phys.*, 1992, **97**, 2635.
- J. Zhou and W. Wang, *Langmuir*, 2000, **16**, 8063-8070.
- J. Schell, N. Casas, R. Pini and M. Mazzotti, *Adsorption*, 2011, **18**, 49-65.
- X. He and M.-B. Hägg, *J. Membr. Sci.*, 2011, **378**, 1-9.
- C. A. Grande, R. Blom, A. Möller and J. Möllmer, *Chemical Engineering Science*, 2013, **89**, 10-20.
- J. Cox, D. D. Wagman and V. A. Medvedev, *CODATA key values for thermodynamics*, Chem/Mats-Sci/E, 1989.
- M. Sevilla and A. B. Fuertes, *J. Colloid Interface Sci.*, 2012, **366**, 147-154.